Journal of Applied Biology & Biotechnology Vol. 14(3), pp. 173-185, May-June, 2026
Available online at http://www.jabonline.in
DOI: 10.7324/JABB.2026.285493

CaECM21 (ORF19.4887), a novel arrestin-related trafficking adaptor involved in nutrient transporter endocytosis and stress adaptation of *CaGAP1* in *Candida albicans*

S Haseena[1,2], Sarika Sharma[3], Kongara Hanumantha Rao[1,4]*

[1]Center of Multidisciplinary Unit of Research on Translational Initiatives (MURTI), GITAM (Deemed to be University), Visakhapatnam, India.
[2]Department of Biotechnology, School of Bioengineering and Biosciences, Lovely Professional University, Phagwara, Punjab, India.
[3]Department of Sponsored Research, Division of Research and Development, Lovely Professional University, Phagwara, Punjab, India
[4]Department of Life Sciences, School of Sciences, Gandhi Institute of Technology and Management (GITAM Deemed to be University), Visakhapatnam, India

ARTICLE INFO

Article history:
Received on: 21/11/2025
Accepted on: 09/03/2026
Available online: 05/04/2026

Key words:
Candida albicans,
CaECM21,
Arrestin-related trafficking adaptor,
CaGAP1,
Endocytosis,
Amphotericin B,
Nutrient transporters.

ABSTRACT

Arrestin-related trafficking (ART) proteins regulate endocytosis and turnover of nutrient transporters in fungi, yet their functional roles in *Candida albicans* remain largely unexplored. In this study, we identified and characterized ORF19.4887, annotated as *CaECM21* in the *Candida* genome database, as a novel ART adaptor protein homologous to *Saccharomyces cerevisiae Rod1*. Sequence analysis revealed conserved PPxY motifs predicted to mediate interaction with the ubiquitin ligase *Rsp5*, suggesting a role in transporter endocytosis. In this study, we characterized *CaECM21* by generating wild-type, mutant, and complemented strains and assessing growth under glucose, *N*-acetylglucosamine (GlcNAc), and amino acid starvation conditions. Transporter localization was examined through GFP fusions and fluorescence microscopy, with quantitative analyses validated by analysis of variance and *post hoc* testing, and amphotericin B (Amp B) sensitivity was evaluated using spot assays. Deletion of *CaECM21* did not result in severe growth defects on glucose and only a moderate reduction in GlcNAc, indicating a condition-specific and modest contribution to nutrient adaptation. Our findings suggest that *CaECM21* modulates nutrient transporter dynamics in response to starvation cues, potentially through ART-like PPxY motifs. Confocal imaging of GFP-tagged transporters demonstrated defective internalization of *CaGAP1* in the Δ/Δ*Caecm21* strain under starvation, confirming a trafficking role for *CaECM21* in transporter internalization. The mutant exhibited increased sensitivity to Amp B, linking ART-mediated trafficking to membrane stress adaptation. This study reveals *CaECM21* as a novel ART adaptor that contributes to nutrient-sensing and antifungal stress tolerance in *C. albicans*. While direct biochemical evidence for *CaECM21-RSP5* remains to be established, this study provides a foundation for future mechanistic and therapeutic investigations into ART-mediated regulation of fungal physiology.

1. INTRODUCTION

Candida albicans is a leading human fungal pathogen, responsible for nearly 70% of hospital-acquired fungal infections and ranked as the fourth most common cause of central line-associated bloodstream infections [1,2]. While *C. albicans* is the most frequently isolated species, other non-albicans *Candida* spp. (*Candida parapsilosis*, *Candida tropicalis*, *Candida krusei*, Candida *glabrata*, *Candida dubliniensis*, *Candida lusitaniae*, and the emerging *Candida auris*) also contribute to clinical infections, with varying antifungal resistance profiles [3]. The clinical impact of *C. albicans* is particularly severe in immunocompromised individuals, including patients undergoing chemotherapy, transplantation, and those suffering from acquired immunodeficiency syndrome [4].

*Corresponding Author:
Kongara Hanumantha Rao,
Center of Multidisciplinary Unit of Research on Translational Initiatives (MURTI), GITAM (Deemed to be University), Visakhapatnam, India.
E-mail: hanu106 @ yahoo.co.in

The pathogenic success of *C. albicans* is linked to its ability to undergo morphological transitions and to metabolize diverse host nutrients. The yeast-to-hypha switch promotes tissue invasion, dissemination, and biofilm formation [5,6], while metabolic plasticity enables survival across distinct host niches [7]. Among host nutrients, N-acetylglucosamine (GlcNAc) is crucial as it serves both as a carbon source and as a potent inducer of hyphal growth [8-10]. Further, amino acids provide nitrogen, modulate morphogenesis, and influence antifungal susceptibility [11-13].

Nutrient uptake in fungi is tightly regulated not only at the transcriptional level but also through post-translational mechanisms controlling transporter abundance at the plasma membrane. In *Saccharomyces cerevisiae*, this regulation is mediated by arrestin-related trafficking (ART) adaptor proteins, which recruit the ubiquitin ligase Rsp5 to target transporters for ubiquitination and endocytosis [14,15]. Similar mechanisms are emerging in *C. albicans*. For instance, the GlcNAc transporter Ngt1 undergoes ubiquitin-dependent endocytosis in response to sugar availability [16,17], while the broad-specificity

amino acid permease *CaGAP1* plays a dual role in nitrogen acquisition and virulence [12,13].

Despite the importance of carbon and nitrogen uptake, the ART proteins coordinating transporter turnover in *C. albicans* remain poorly characterized. *In silico* analysis of ORF19.4887, designated as *CaECM21*, revealed a conserved arrestin domain and PPxY motifs predicted to interact with Rsp5, suggesting a role in endocytosis. Recent studies in *Cryptococcus neoformans* and *Aspergillus fumigatus* have demonstrated that ART-domain proteins contribute to transporter regulation and antifungal tolerance [18,19]. These findings imply a conserved role of arrestin-like proteins in fungal adaptability and drug response.

Comparative sequence analyses further indicate that *CaECM21* shares structural features with its orthologs *Rod1* in *S. cerevisiae*, *ArtA* in *A. fumigatus*, and arrestin-like proteins in *C. neoformans*, all containing characteristic arrestin-C domains and PPxY motifs. This evolutionary conservation suggests that ART-mediated trafficking is an ancient and fundamental mechanism for maintaining plasma membrane homeostasis across fungal species.

Based on these insights, we hypothesized that *CaECM21* regulates the endocytosis of nutrient transporters such as *CaGAP1*, thereby integrating carbon and nitrogen sensing in *C. albicans*. To investigate the endocytic process, we employed a combination of in silico, molecular, and cell biological approaches. These included generating homozygous *CaECM21* gene deletion, C-terminal GFP-tagging, fluorescence microscopy under defined nutrient conditions, and antifungal susceptibility assays. This study provides the first experimental evidence establishing *CaECM21* as a functional ART adaptor protein in *C. albicans,* linking nutrient transporter trafficking to stress adaptation and antifungal response.

2. MATERIALS AND METHODS

2.1. Strains and Culture Conditions

All experiments were performed using the *C. albicans* laboratory strain BWP17, which is auxotrophic for uridine, histidine, and arginine [Table 1]. Strains were maintained as glycerol stocks at −80°C and freshly streaked onto YPD agar plates (1% yeast extract, 2% peptone, 2% dextrose, 2% agar; HiMedia) before experimentation. Plates were incubated at 30°C for 48 h, and single colonies were used to initiate cultures. For routine propagation, cells were grown in YPD broth (1% yeast extract, 2% peptone, 2% glucose, w/v) at 30°C with shaking (200 rpm). Auxotrophic requirements were supplemented with uridine and histidine (20 µg/mL each) and arginine (30 µg/mL; Sigma-Aldrich) [20].

For experimental assays, overnight cultures were diluted into synthetic defined medium and allowed to reach mid-logarithmic phase (optical density $[OD]_{600} \approx 0.6$). Cells were washed twice with YNB basal medium and resuspended in YNB complete and YNB lacking amino acids (W/O aa; Difco), supplemented with glucose or GlcNAc as the sole carbon source [21,22]. Stock solutions of GlcNAc and amino acids were filter-sterilized (0.45 µm) and added aseptically after autoclaving. Growth was routinely monitored by OD_{600} readings, and all experiments were performed in three independent biological replicates, each with three technical replicates. Wild-type, Δ/*ΔCaecm21*, and complemented strains (Δ/*ΔCaecm21*+*CaECM21*) were analyzed in parallel to confirm that observed phenotypes were attributable to *CaECM21* deletion.

Table 1: List of strains and plasmids used to prepare Δ/Δ*CaECM21.*

Strain	Genotype of constructed strains	Source/ reference
Candida albicans strain		
BWP17	*ura3Δ::limm434/ura3Δ::limm434 his1::hisG/ his1::hisG arg4::hisG/arg4::hisG*	Alistair J.P. Brown
HHR1	*ΔCaecm21::HIS1/CaECM21 ura3Δ::* Δ *imm434/ura3Δ::* Δ *imm434 his1::hisG/ his1::hisG arg4::hisG/arg4::his*	This study
HHR2	ΔCaecm21::HIS1/ecmΔ:: ARG4 ura3Δ:: Δ imm434/ura3Δ:: Δ imm434 his1::hisG/ his1::hisG arg4::hisG/arg4::hisG	This study
HHR3	*NGT1-GFPɣ:: URA3/CaECM21 ura3Δ::limm434/ura3Δ::limm434 his1::hisG/ his1::hisG arg4::hisG/arg4::hisG*	This study
HHR4	*pFA-GFPɣ-CaGap1::HIS1/CaGap1 ura3Δ::limm434/ura3Δ::limm434 his1::hisG/ his1::hisG arg4::hisG/arg4::hisG*	This study
HHR5	*pFA-GFPɣ-CaGap1-ecm21Δ::HIS1/ Caecm21Δ**u**ra3Δ::limm434/ura3Δ::limm434 his1::hisG/his1::hisG arg4::hisG/arg4::hisG*	This study
Escherichia coli strains		
pSN52	C.d HIS1, KanR (pCR-Blunt II-TOPO vector (Invitrogen) carrying *HIS1* gene of *Candida dubliniensis*)	Rao *et al*., 2020
pSN69	pCR-Blunt II-TOPO vector (Invitrogen) carrying the *ARG4* gene of *Candida dubliniensis*	Rao *et al*., 2020
pFa-GFPγ-ARG4	plasmid harboring a codon optimized GFPγ, a photostable GFP variant along with the *URA3* marker	Rao *et al*., 2020

PCR: Polymerase chain reaction.

2.2. DNA Sequence Analysis

The *C. albicans* genome (~14.7 Mbp) encodes approximately 6,000 genes [23]. The *ART-domain containing* gene *CaECM21* was selected for functional analysis and targeted for deletion in the BWP17 background. Homology searches using the basic local alignment search tool (BLAST) [24] revealed ~42% identity and ~58% similarity with *S. cerevisiae* Rod1, an ART adaptor protein [Figure 4]. Multiple sequence alignment with CLUSTALW [25] confirmed conservation of the ART domain and identified two PY motifs (PPxY) at residues 215–218 and 459–462, which may serve as binding sites for the ubiquitin ligase Rsp5. Further analysis of the *CaECM21* open reading frame using Restriction Mapper 2.0 identified unique restriction sites suitable for cloning and mutant construction. Conserved domain analysis using the National Center for Biotechnology Information conserved domain database [26] predicted an N-terminal arrestin domain and several low-complexity regions, consistent with a role in adaptor-mediated protein trafficking [27]. All annotations were cross-checked against the *Candida* genome database (CGD) (http://www.candidagenome.org). These analyses guided the selection of *CaECM21* as a candidate ART adaptor potentially involved in the endosomal transport of *CaGap1*.

2.3. Preparation of *CaECM21* Deletion Mutants in *C. albicans*

In this study, deletion of *CaECM21* in the BWP17 strain (gift from Dr. Swagata Ghosh, University of Kalyani) was performed

using polymerase chain reaction (PCR)-mediated homologous recombination [20,28]. The two alleles were sequentially replaced using *HIS1* and *ARG4* markers, amplified from plasmids pSN52 and pSN69, respectively. Disruption cassettes were generated with primers containing 81 bp homology to the upstream and downstream flanking regions of *CaECM21* [Table 2]. Purified cassettes were introduced into electrocompetent BWP17 cells through electroporation. Transformants were recovered in YPD medium containing 1 M sorbitol at 30°C for 2 h and selected on SD agar lacking histidine, producing heterozygous mutants (Δ*Caecm21:HIS1*, designated HHR1). A second round of transformation with the *ARG4* cassette, followed by selection on SD agar lacking arginine, generated homozygous knockouts (Δ/Δ*Caecm21:HIS1/ARG4*, designated HHR2). Allele replacement was confirmed by diagnostic PCR using primers flanking the targeted locus and internal primers spanning the deleted region. Screening of ~40 transformants yielded ~65% correct replacement for the first allele and ~50% for the second. Two independent Δ/Δ*CaECM21* mutants (HHR2-1 and HHR2-2) were retained for downstream phenotypic analyses.

For complementation, a wild-type *CaECM21* fragment, including ~500 bp upstream promoter and ~300 bp downstream terminator, was cloned into a *URA3*-marked integration vector. The construct was linearized and introduced into Δ/Δ*CaECM21* strains by electroporation. Uracil prototrophs were selected on SD-*URA* lacking plates, and correct integration was verified by PCR. Complemented strains (Δ/Δ*CaECM21+CaECM21*) were analyzed alongside wild-type and knockout strains to confirm that observed phenotypes were attributable to *CaECM21* deletion. A schematic representation of the deletion and complementation strategy is depicted with a schematic diagram [Figure 1].

2.4. Spot-Dilution Assay of GlcNAc-Induced Δ/Δ*Caecm21* Cells

To assess the nutrient-specific growth, wild-type (BWP17), double mutant (Δ/ΔCaecm21), and complemented strains (ΔCaecm21) were grown overnight in YPD, washed with YNB basal medium, and adjusted to OD_{600} = 1. Serial dilutions (10^{-1} to 10^{-4}) were spotted (10 µL) onto YNB-glucose and YNB-GlcNAc plates and incubated at 30°C for 24 h. Growth patterns were documented, and colony area was quantified using ImageJ [Figure 2]. All data represent mean±SD of triplicate biological repeats. Statistical significance was determined using one-way analysis of variance (ANOVA) followed by Tukey's *post hoc* test ($P < 0.05$) [21].

2.5. Microscopic Study of GlcNAc-Induced Δ/Δ*Caecm21* Cells

C. albicans strains were freshly revived on YPD agar, and a single colony was inoculated into 5 mL YPD broth. Cultures were incubated overnight at 30°C. The following day, 1% of the overnight culture was

Table 2: Primers used for *CaECM21* deletion, confirmation, and GFP tagging in *Candida albicans*.

Primer Name	Sequence (5'–3')	Number of base pairs	Use of Primer	Genotype/construct
Caecm21-Del-F	GAACCATCAATCTTGGAA ATCGCAGCCACCAATTCTCAAA ATAAATCGAGAAGGCTA AGTAGCTCGGATCCACTAGTAACG	81	Amplification of the upstream flank for *Caecm21* deletion	Δ*Caecm21* (single knockout mutant)
Caecm21-Del-R	ATTACCACAAAATTTCATTA AAAATACAAAATTAAATATA AATTACAAGATAAATTAATAG CCAGTGTGATGGATATCTGC	81	Amplification of the downstream flank for *Caecm21* deletion	Δ*Caecm21* (single mutant)
Caecm21-check-F	TTATTTCCTTGTGGATGTCC	20	Confirmation of *Caecm21* deletion (forward)	Δ*Caecm21* single mutant (confirmation)
Caecm21-check -R	TATCGTGACTATTCTGATGG	20	Confirmation of *Caecm21* deletion (reverse)	Δ*Caecm21* single mutant (confirmation)
His-check.R	ATCAGATGGGTTATCTCGTC	20	Confirmation of *HIS1* marker insertion	Δ*Caecm21::HIS1* mutant
ARG4-check-R	TGGTTCAGGTAGATATTCCT	20	Confirmation of *ARG4* marker insertion	Δ/Δ*Caecm21::HIS1/ARG4* double mutant
Ngt1-GFP-F	ACCCCCATCGTTTTACTT AGTTCAAAATGTCAAGAAG ATTCTCCTCCTTATAGTTCT GTAGGTGCTGGCGCAGGTGCTTC	80	C-terminal tagging of Ngt1 using plasmid pFA-GFPγ-URA in both BWP17 and Δ/Δ*Caecm21* (forward primer)	Ngt1- GFPγ (BWP17) and Ngt1- GFPγ (Δ/Δ*Caecm21*) tagged strain
Ngt1-GFP-R	AAAATTACCACAAAATTT CATTAAAAATACAAATTAAAT ATAAATTACAAGATAAATTA ATATCTGATATCATCGATGAATTCGAG	86	C-terminal tagging of Ngt1 using plasmid pFA-GFPγ-URA in both BWP17 and Δ/Δ*Caecm21* (reverse primer)	Ngt1- GFPγ (BWP17) and Ngt1- GFPγ (Δ/Δ*Caecm21*) tagged strain
CaGap1-GFP-F	AGATTTGTTACAACAAGAAA TAGCTGAAGAAAAAGCTC AATTAGCTGAAAAACCATTC TATATGGTGCTGGCGCAGGTGCTTC	83	C-terminal tagging of CaGap1 using plasmid pFA-GFPγ-URA in both BWP17 Δ/Δ*Caecm21* (forward primer)	*Ca*Gap1-GFPγ (BWP17) and CaGap1- GFPγ (Δ/Δ*Caecm21*) tagged strain
CaGap1-GFP-R	ACTATATATATTAAGTATCA AAATTTGTCTATCTATTATTTTTAGCAC CAAAATCTATAAATTTCTGATAT CATCGATGAATTCGAG	87	C-terminal tagging CaGap1 using plasmid pFA-GFPγ-URA in both BWP17 Δ/Δ*Caecm21* (reverse primer)	CaGap1-GFPγ (BWP17) and *Ca*Gap1- GFPγ (Δ/Δ*Caecm21*) tagged strain

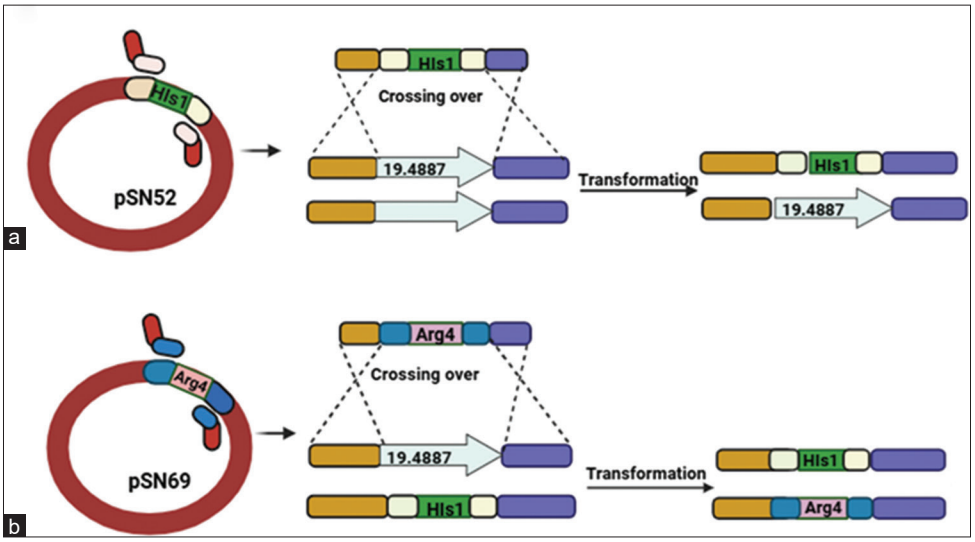

Figure 1: Schematic representation of *CaECM21* (ORF19.4887) gene deletion and generation of the homozygous knockout strain in *Candida albicans*. (a) The first allele of *CaECM21* was disrupted using a deletion cassette derived from plasmid pSN52 carrying the *HIS1* marker. Homologous recombination in the BWP17 strain replaced one copy of the *CaECM21* locus with *HIS1*, and transformants were selected on SD medium lacking histidine and verified by diagnostic polymerase chain reaction (PCR). (b) The second allele was deleted using a cassette from plasmid pSN69 containing the *ARG4* marker, transformed into the heterozygous strain. Transformants were selected on SD medium lacking arginine, and successful homozygous deletion mutants were confirmed by PCR analysis.

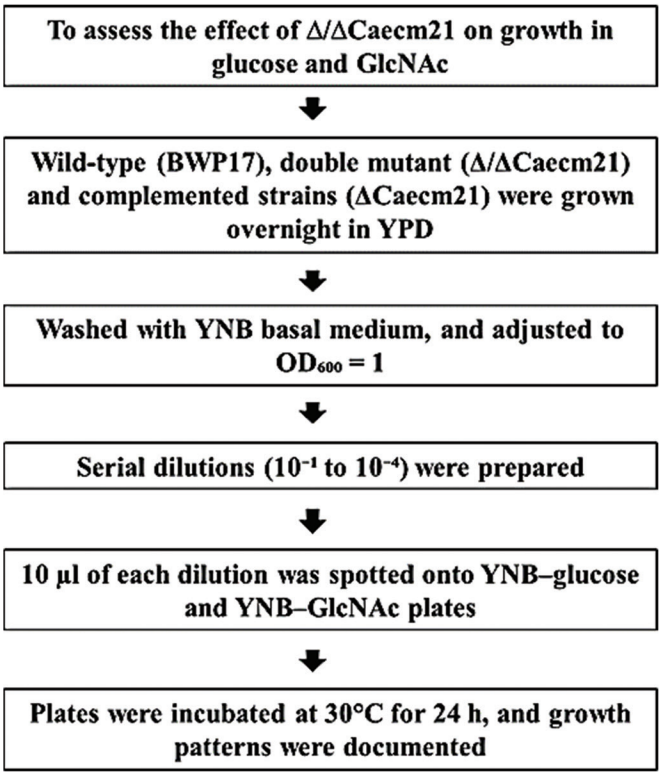

Figure 2: Experimental workflow to assess the effect of glucose and GlcNAc on growth in *Candida albicans* strains. Spot assay of *C. albicans* strains on glucose and GlcNAc. Serial dilutions of wild-type, mutant, and complemented strains were spotted on YNB plates with glucose or GlcNAc and incubated at 30 °C for 24 h.

transferred into fresh YPD broth and grown to mid-logarithmic phase (OD_{600} ≈ 0.4). Cells were harvested by centrifugation, washed twice with YNB basal medium, and resuspended in YNB supplemented with glucose and GlcNAc. Cultures were incubated at 30°C for 2 h to induce morphological changes [Figure 5b] [29].

2.6. Epitope Tagging

C-terminal GFPγ tagging of *Ngt1* and *CaGAP1* proteins using a PCR-based strategy was performed in both BWP17 and Δ/Δ*Caecm21* backgrounds using plasmid pFA-GFPγ-URA [30,31]. PCR cassettes with ~80 bp homology were electroporated into competent cells. Transformants were selected on SD-*URA* lacking plates, and integration was verified by PCR [Figure 3]. For bright-field microscopy, 5 µL of each cell suspension was mounted on a glass slide, covered with a coverslip, and observed using a Nikon 80i inverted microscope equipped with a Nikon DXM1200C digital camera [Figure 6a]. For fluorescence microscopy of Ngt1-GFPγ and CaGap1-GFPγ expressing cells, imaging was performed using an Olympus confocal microscope with a C-Apochromat ×60/1.2 numerical aperture objective. GFP was excited at 488 nm (range 440–475 nm) and emission was detected at 509 nm (range 500–540 nm) using the appropriate GFP/FITC filter set. The focal plane was positioned at the midsection of the cells to ensure accurate intracellular localization. Untagged controls were used as negative controls for autofluorescence and background signal. GFP-tagged strains in a wild-type background served as positive controls to ensure that fluorescence reflected specific transporter localization rather than artifacts of tagging [Figure 6b].

2.7. Impact of Glucose and GlcNAc on *CaGap1* and Functional Assessment of *CaECM21*

To investigate the effect of nutrient conditions on *CaGap1* localization and to assess the role of CaECM21, wild-type (BWP17) and Δ/Δ*Caecm21* strains carrying CaGap1-GFPγ were cultured overnight in YPD at 30°C. Cells were washed twice with YNB basal medium and resuspended in YNB supplemented with both 2% glucose and 2% GlcNAc, with or W/O aa [32]. Untagged strains were used as negative controls to exclude autofluorescence, and images were processed using ImageJ [Figure 7].

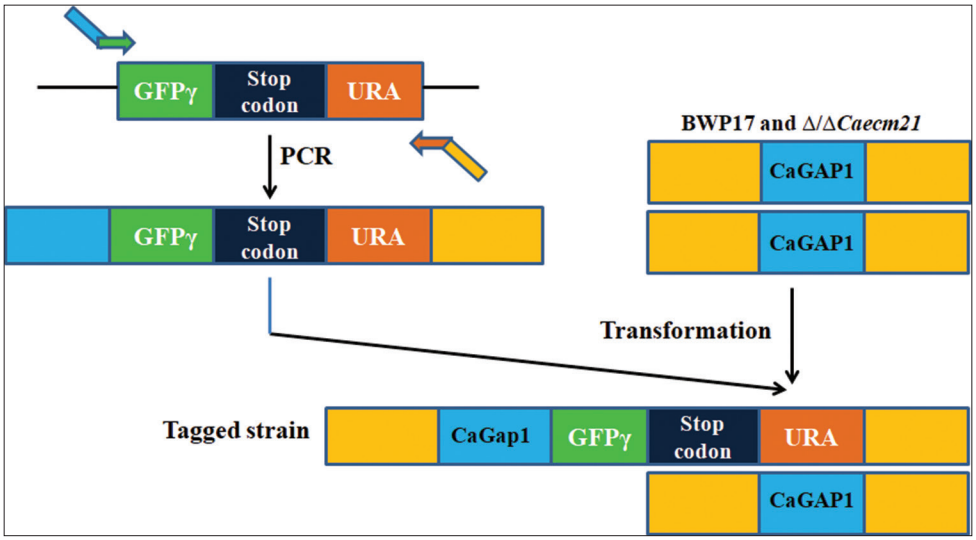

Figure 3: Schematic overview of C-terminal GFPγ tagging of *CaGAP1* in *Candida albicans* wild-type and Δ/ΔCaecm21 strains. A tagging cassette containing GFPγ, a stop codon, and the *URA3* marker was amplified from plasmid pFA-GFPγ-URA and integrated at the 3′ end of the *CaGAP1* ORF by homologous recombination. Transformants were selected on *URA*-lacking medium and confirmed by diagnostic polymerase chain reaction. The resulting CaGap1-GFPγ strains were used for fluorescence microscopy to study protein localization under different carbon source conditions.

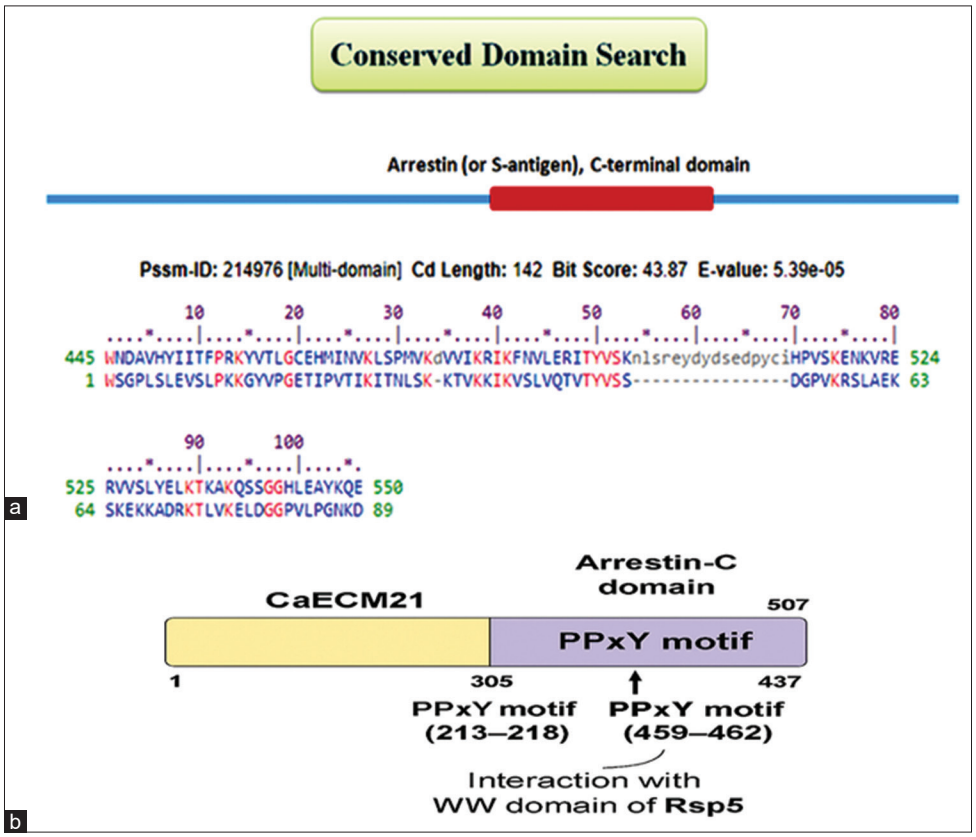

Figure 4: Structural and functional representation of *CaECM21* in ubiquitin-mediated endocytosis. (a) A conserved domain search revealed that *CaECM21* in *Candida albicans* contains an Arrestin-C domain, similar to Rod1 (ORF19.1509), which also harbors a PPxY motif essential for Rsp5 interaction. BLASTP analysis identified *CaECM21* as structurally related to Rod1, suggesting its potential role in regulating plasma membrane transporter internalization, possibly targeting *Ngt1* and *CaGap1* for endocytic turnover. (b) Schematic diagram of the *C. albicans*, CaEcm21 protein, highlighting key domains and motifs. The protein contains an Arrestin-C domain and two PPxY motifs located at amino acid positions 213–218 and 459–462, which mediate interaction with the WW domain of the E3 ubiquitin ligase Rsp5.

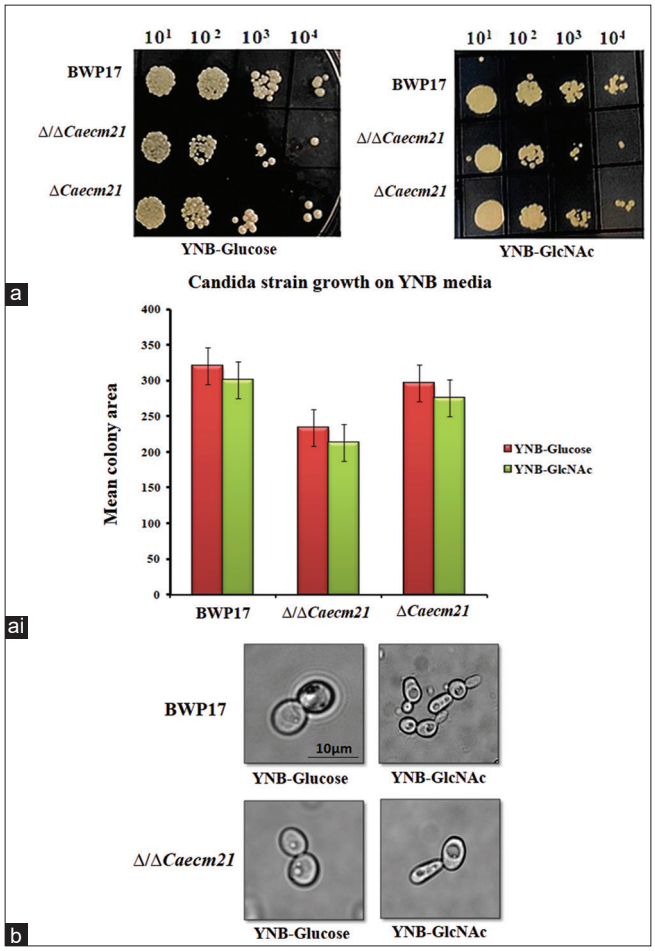

Figure 5: Growth and morphological responses of wild-type, Δ/ΔCaecm21, and complemented strains under glucose and GlcNAc conditions. (a) Spot assay of BWP17, double mutant (Δ/Δ*Caecm21*) and complementary strains (Δ*Caecm21*) on YNB-glucose and YNB-GlcNAc. (a i) Quantitative growth analysis using integrated density measurements from four biological replicates (n = biological replicates [4], analysis of variance, $P < 0.0001$), Image J tool. (b) Microscopic examination of yeast-to-hyphal transition under glucose and GlcNAc after 2 h of induction. Scale bar: 10 µm.

2.8. Localization of *CaGap1* under Nutrient Conditions

CaGap1 is a broad-spectrum aa transporter in *C. albicans*, essential for nitrogen acquisition and nutrient sensing [32]. To assess its expression and trafficking, wild-type and Δ/Δ*Caecm21* strains expressing CaGap1-GFPγ were grown overnight in YPD. Cells were washed twice and induced under four conditions: YNB + glucose, YNB + GlcNAc, YNB W/O aa + glucose, and YNB W/O aa + GlcNAc. Samples were collected at 60 min and 120 min for fluorescence microscopy. Localization patterns (membrane, cytoplasmic, vacuolar) were quantified using Image J [Figure 8] [33].

2.9. Amphotericin B Sensitivity Assay

As *CaEcm21* is observed to be involved in endosomal trafficking of membrane proteins like *CaGap1*, we wanted to check the sensitivity of mutant cells against the Amp B. Amp B is reported to bind to ergosterol moieties of the cell membrane, affecting the endocytic pathway [33]. Amphotericin B (Amp B) is widely recognized as a highly effective antifungal agent used to treat severe fungal infections [34]. Numerous investigations have highlighted the remarkable potency of Amp B in combating fungal pathogens [35,36]. We further investigated whether *CaECM21* contributes to antifungal stress tolerance by testing sensitivity to Amp B. In particular, we assessed sensitivity to Amp B, a clinically relevant polyene that disrupts ergosterol-containing membranes. The susceptibility of *C. albicans* strains to amphotericin B (Amp B) was assessed by spot assay under four conditions: YNB + dimethyl sulfoxide (DMSO) (WC), YNB culture, 0.7 µg/mL Amp B, and 12 µg/mL Amp B. On control plates (YNB + DMSO, WC) and on YNB culture plates, wild-type, Δ/Δ*Caecm21* and the complemented strain displayed comparable growth, indicating that neither the vehicle (DMSO) nor the culture filtrate affected basal viability [37]. Wild-type, Δ/Δ*Caecm21*, and complemented strains were grown overnight in YPD at 30°C, washed twice with Milli-Q water. Cell suspensions were adjusted to OD_{600} = 0.4 in sterile water, and ten-fold serial dilutions were prepared. 5 µL of each dilution was spotted onto YNB-GlcNAc agar plates supplemented with either 0.7 µg/mL or 12 µg/mL Amp B. YNB medium without drug was used to monitor basal growth, while YNB + DMSO was included as a vehicle control. Plates were incubated at 30°C for 48–72 h, and growth differences were documented. Spot intensity and colony size were quantified using ImageJ. Data represent averages from three independent biological replicates, and statistical analysis was performed by one-way ANOVA (Tukey's *post hoc*, $P < 0.05$).

2.10. Fluorescence Quantification and Statistical Analysis

Quantitative analysis was performed using ImageJ (version 1.53; NIH, USA). Individual cells were segmented automatically using threshold-based region of interest selection, and mean fluorescence intensity (MFI) [Table 3] was calculated after subtracting background from cell-free regions. Each field contained ≥30 cells, and at least 3 fields were analyzed per replicate. Fluorescence data were represented as averages from three independent biological replicates as mean ± standard deviation (SD). For each comparison, 95% confidence intervals (CIs) and exact *P*-values were calculated to ensure statistical transparency. Brightness and contrast adjustments were applied uniformly to representative images using Adobe Photoshop version 5.5 (Adobe Systems, San Jose, CA). Statistical analyses were performed using GraphPad Prism 10, which was used for one-way or two-way ANOVA with Tukey's *post hoc* tests. Results were considered significant thresholds as $P < 0.05$ [Figure 6 bi].

3. RESULTS AND DISCUSSION

3.1. In silico Identification of ART Domain-Containing Proteins in *C. albicans*

To identify ART domain-containing proteins potentially involved in ubiquitin-mediated endocytosis, a BLASTp search was performed in CGD using the α-arrestin *Rod1* (C2_01970C_A) as the query. Rod1 mediates internalization of plasma membrane transporters through interaction with the ubiquitin ligase *Rsp5*. Sequence analysis of *C. albicans* SC5314 Assembly 22 revealed a previously uncharacterized paralog, *CaECM21* (C1_10180C_A), sharing 24.63% sequence identity with *Rod1* across the conserved arrestin domain (E-value = 2e-10) [Figure 4]. Conserved domain analysis revealed two PPxY motifs (residues 213–218 and 459–462) predicted to interact with the WW domain of the ubiquitin ligase *Rsp5*. Such motifs are essential for ubiquitin-mediated endocytosis in *S. cerevisiae* and other fungi [38]. In silico predictions suggest that *CaECM21* could function as a putative ART adaptor facilitating the internalization of nutrient transporters such as *Ngt1* and *CaGAP1*.

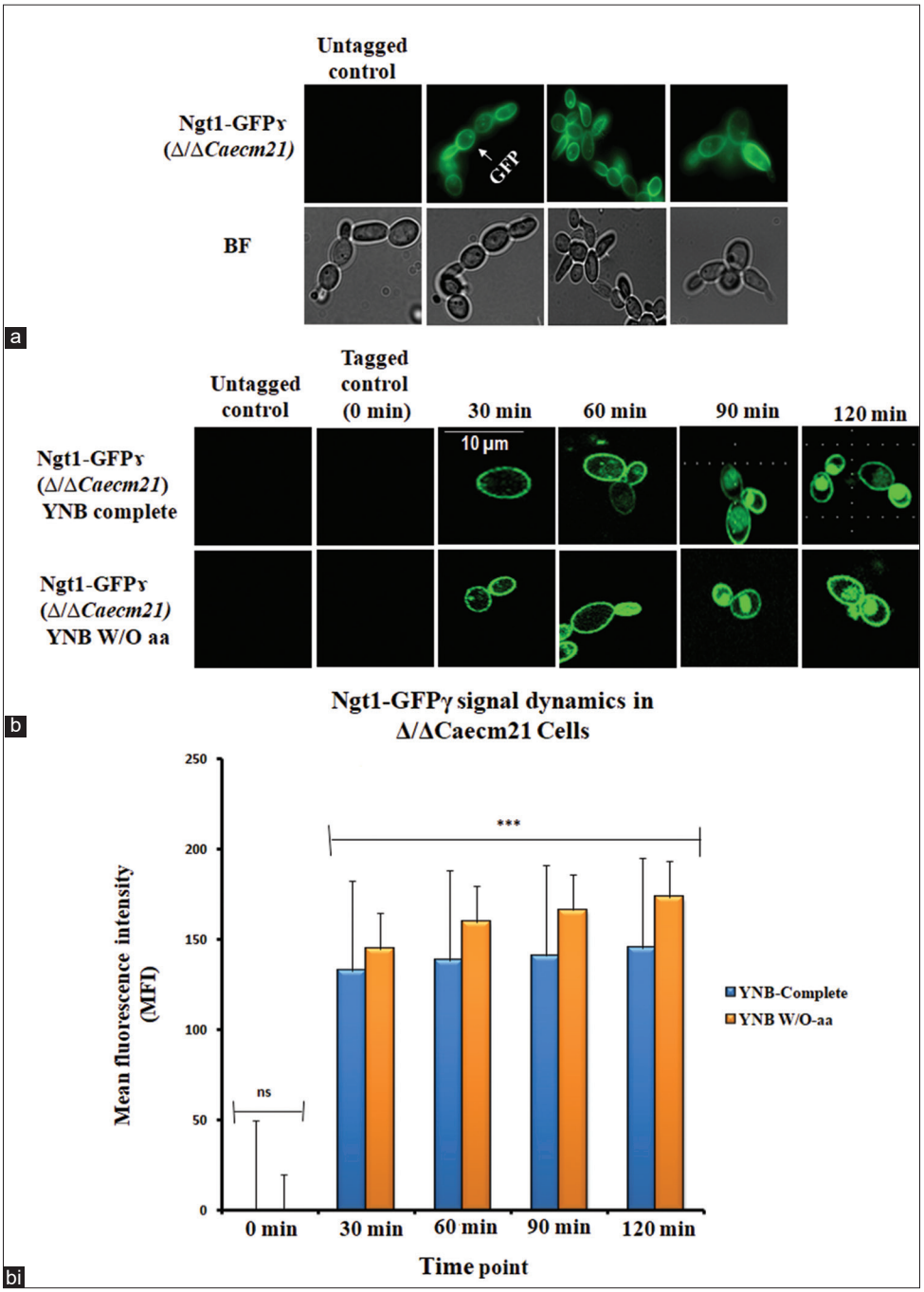

Figure 6: GlcNAc-induced localization dynamics of Ngt1-GFPγ in Δ/Δ*Caecm21 cells*. (a) Fluorescence microscopy of Ngt1-GFPγ in ΔΔCaecm21 cells under GlcNAc induction. BF = bright field. (b) Time-course panels showing subcellular localization at 0, 30, 60, 90, and 120 min, Scale bar: 10 µm. (b i) Bar graph showing mean fluorescence intensity (MFI) of Ngt1-GFPγ under two nutrient conditions: YNB complete (blue) and YNB W/O-aa (orange). Fluorescence was undetectable at 0 min in both conditions (ns). From 30 min onward, MFI increased progressively in both media, with consistently higher values observed in YNB W/O-aa. Error bars represent standard deviation (SD) from three biological replicates ($n = 3$). Statistical significance was determined using Tukey's *post hoc* test following two-way analysis of variance ($P < 0.001$, ns = not significant).

3.2. Characterization of the Δ/ΔCaecm21 Deletion Mutant

The mutant was characterized for growth on different carbon sources, including glucose and GlcNAc, in the presence and absence of aa using spot assays. Additionally, cell morphology was assessed under glucose and GlcNAc-inducing conditions. Localization studies of *CaGap1* were performed to investigate the role of CaEcm21 in endosomal trafficking. The Δ/Δ*Caecm21* mutant was also tested for sensitivity to the antifungal agent amphotericin B. These analyses provide the first evidence that *CaECM21*, an ART-family protein, contributes to the endosomal trafficking of *CaGap1*. Notably, CaGap1-GFPγ expression is sensitive to YNB-GlcNAc and displays membrane localization in the presence of aa, supporting the role of CaEcm21 in regulating nutrient transporter trafficking.

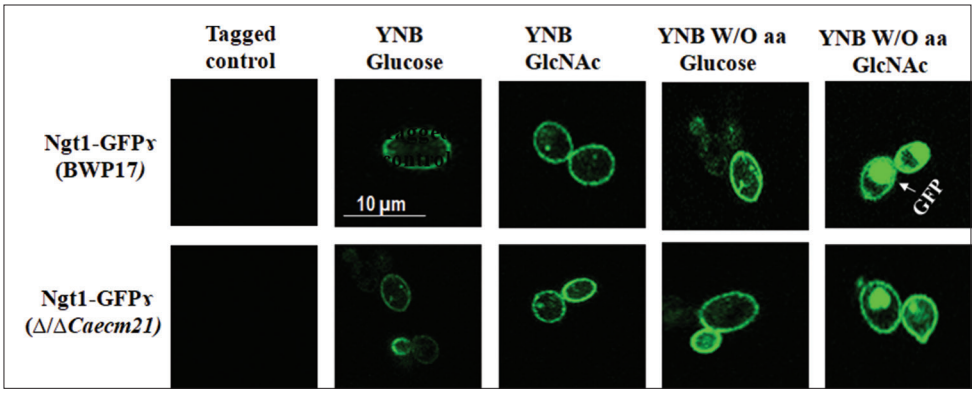

Figure 7: Nutrient-dependent localization of CaGap1-GFPγ in *Candida albicans*. Fluorescence microscopy of wild-type (BWP17) and Δ/ΔCaecm21 strains grown in YNB with glucose or GlcNAc, with or without amino acids. Amino acid starvation enhanced *CaGap1* internalization with a strong vacuolar signal in GlcNAc-grown wild-type cells, whereas the mutant retained membrane-associated fluorescence. Scale bar = 10 µm.

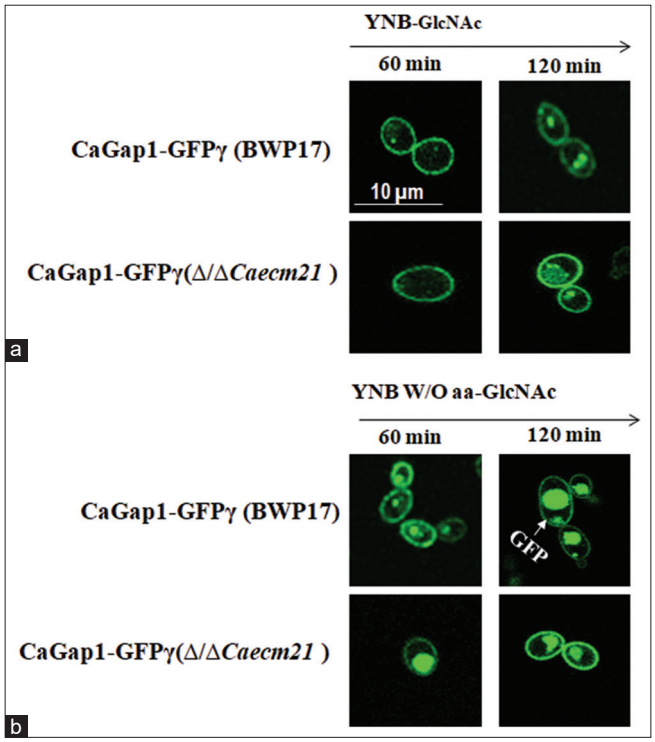

Figure 8: Time-dependent localization of CaGap1-GFP in *Candida albicans* under GlcNAc conditions. (a) Fluorescence microscopy images of wild-type (BWP17) and Δ/Δ*Caecm21* strains expressing CaGap1-GFPγ were cultured in YNB medium supplemented with GlcNAc and examined after 60 and 120 min. Both strains showed peripheral GFP fluorescence at both time points. (b) Cells grown in YNB W/O aa plus GlcNAc were analyzed at 60 and 120 min. Under amino acid starvation, GFP signal increased over time, with pronounced vacuolar accumulation in BWP17 cells at 120 min (arrow), while the Δ/Δ*Caecm2*1 strain displayed altered localization.

3.3. Growth and Morphogenesis of *CaECM21* Mutant Strains

To assess the role of CaEcm21 in *C. albicans* growth on glucose and GlcNAc media, spot assays were performed using the wild-type strain BWP17, double mutant (Δ/Δ*Caecm21)*, and complemented strains (Δ*Caecm21*) [Figure 5a]. All strains were able to grow under both conditions, while Δ/Δ*Caecm21* strains showed reduced growth both on glucose and GlcNAc plates, as shown in the bar diagram [Figure 5a i] and the statistical analysis [Table 4, $P < 0.0001$]. This indicates a condition-specific contribution of *CaECM21* to nutrient adaptation.

Table 3: Data are mean±SD of three independent replicates, significance determined by two-way analysis of variance with Tukey's *post hoc* test.

Time (min)	YNB complete (mean±SD)	YNB W/O-aa (mean±SD)	Significance (Tukey HSD)
0	0.0±0.0	0.0±0.0	NS
30	132.7±0.7	144.5±0.8	***
60	138.2±0.4	159.5±0.6	***
90	141.0±0.7	166.2±0.9	***
120	145.2±0.3	173.4±0.8	***

SD: Standard deviation, NS: Non-significance. ***$P < 0.001$ (highly statistically significant)

To further investigate the role of *CaECM21* in morphogenetic transition, cells were induced in YNB-glucose and YNB-GlcNAc media for 2 h, and morphological changes were examined microscopically. Cells grown in glucose predominantly retained a yeast-like morphology, whereas GlcNAc-induced cells formed mycelia in both wild-type and mutant strains, with no notable differences in morphological changes [Figure 5b]. These findings suggest that *CaECM21* contributes to efficient growth and GlcNAc-induced morphogenesis, although its absence reduces the overall response.

3.4. Plasma Membrane Localization of GlcNAc-Induced *Δ/ΔCaecm21*

To determine whether membrane transporters' localization correlates with *CaECM21* predicted role in endosomal trafficking of nutrient transporters, the fusion protein was examined under GlcNAc-inducing conditions (YNB-GlcNAc) using fluorescence microscopy. Under these conditions, Ngt1-GFPγ localized predominantly to the plasma membrane [Figure 6a]. These observations provide the first experimental evidence for GlcNAc-dependent plasma membrane localization of *Ngt1* in *C. albicans* and are consistent with previous studies employing similar GFP-tagging approaches [34].

3.5. Ngt1-GFPγ Localization under Amino Acid Limitation

To investigate the time-dependent relocalization of *Ngt1* in Δ/Δ*Caecm21* cells, cultures were grown overnight and incubated with

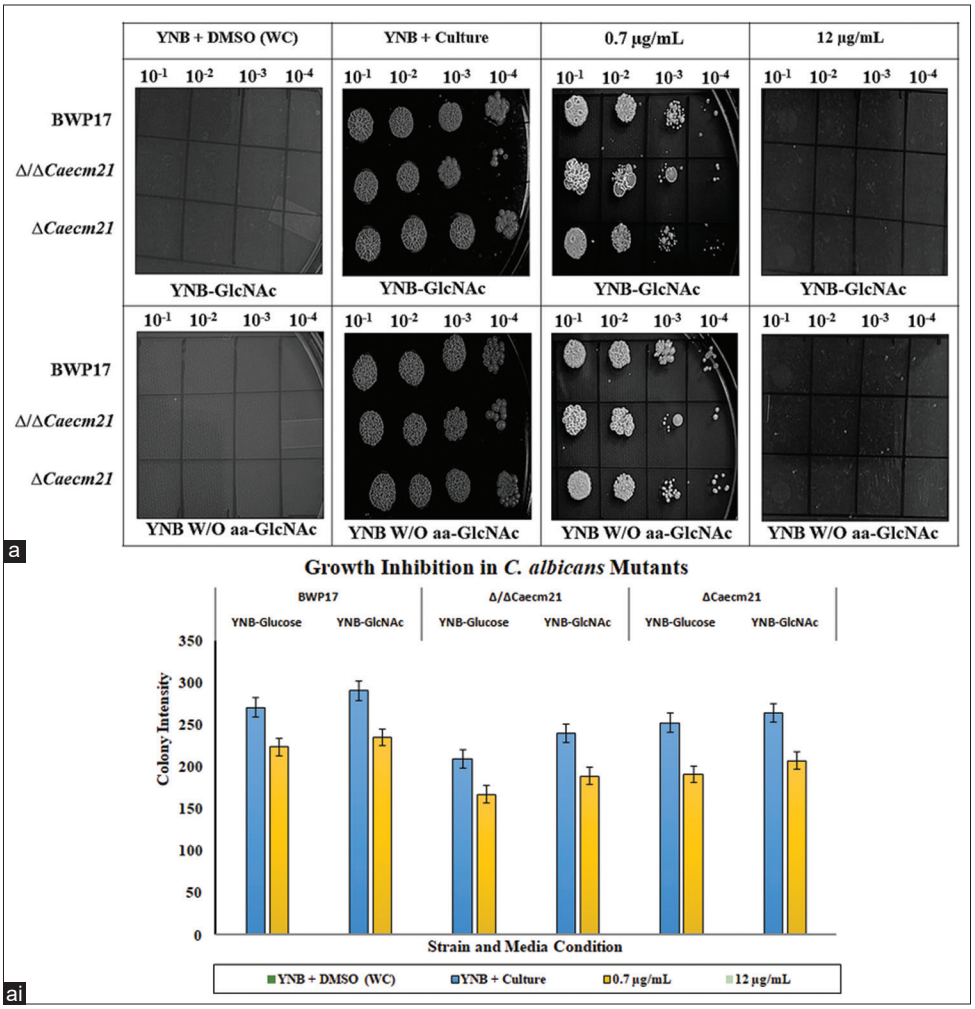

Figure 9: Antifungal spot assay of amphotericin B (Amp B) against *Candida albicans* strains. (a) Wild-type, Δ/Δ*Caecm21*, and complemented strains were spotted in ten-fold serial dilutions (10^{-1} to 10^{-5}) onto YNB-GlcNAc agar plates under four conditions: YNB + DMSO (without-drug control, WC), YNB culture, 0.7 µg/mL Amp B, and 12 µg/mL Amp B. Plates were incubated at 30°C for 48–72 h, and growth patterns were documented. Representative images are shown (upper panel). (a i) Quantitative analysis of colony size and spot intensity (integrated density) was performed using ImageJ from three independent biological replicates (lower panel). Data are presented as mean±standard deviation (SD), and statistical significance was assessed using one-way analysis of variance with Tukey's *post hoc* test (P < 0.05).

Table 4: Mean colony area of *Candida albicans* strains grown on YNB-glucose and YNB-GlcNAc media.

Strain	YNB-glucose (mean±SD)	95% CI	*P* versus WT	YNB-GlcNAc (mean±SD)	95% CI	*P* versus WT
BWP17	320.4±8.1	(307.5, 333.3)	Reference	300.3±6.0	(290.7, 309.9)	Reference
Δ/ΔCaecm21	234.2±5.5	(225.5, 242.9)	0.0007	213.3±5.4	(204.7, 221.9)	0.0011
ΔCaecm21	296.3±5.9	(286.9, 305.7)	0.039	275.1±6.2	(265.2, 285.0)	0.041

SD: Standard deviation, CI: Confidence interval.

YNB-GlcNAc and YNB W/O aa-GlcNAc conditions. All fluorescence pictures were observed under the epifluorescence microscope at different time intervals. Importantly, no detectable fluorescence was observed in untagged strains, confirming that signals originated specifically from GFP-tagged transporters. Tagged mutant strains at 0 min served as negative controls and showed no signal. Interestingly, between 30 and 60 min, fluorescence appeared at the plasma membrane, indicating transporter activation. At 90 min, internal puncta were visible, and at 120 min, fluorescence was predominantly vacuolar, suggesting endocytic trafficking [Figure 6b].

Quantitative analysis of MFI confirmed these localization dynamics across three biological replicates [39]. Cells grown in YNB W/O-aa consistently exhibited higher MFI than those in YNB complete medium at all time points beyond 0 min. The observation was compared across conditions using two-way ANOVA followed by Tukey's *post hoc* test [$P < 0.001$, $n = 3$, Table 3]. The statistical analysis validated the observed differences in transporter localization, confirming that trends were not due to random variation. These results support the hypothesis that *CaECM21* acts as an ART adaptor promoting nutrient-dependent transporter internalization [Figure 6b i].

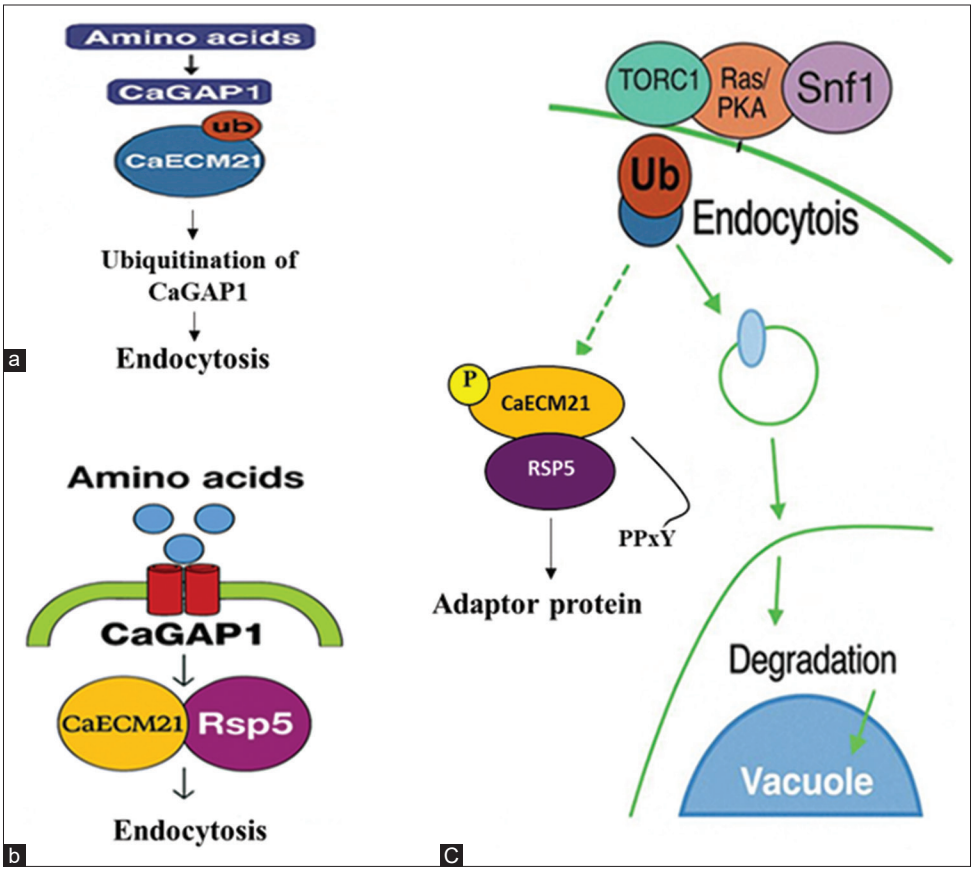

Figure 10: Model Figure representing *CaECM21* in the regulation of *CaGAP1* endocytosis under nutrient-rich and nutrient-limited conditions in *Candida albicans.* (a) Under nutrient-rich conditions, *CaGAP1* remains stable at the plasma membrane and mediates amino acid uptake, with minimal ubiquitination and limited endocytosis. (b) During nutrient limitation, *CaECM21* contains two conserved PPxY motifs (213–218 and 459–462) that recruit the E3 ubiquitin ligase *Rsp5*, leading to ubiquitination of *CaGAP1* and its endocytosis and triggering its internalization. (c) Integrated schematic showing nutrient-signaling pathways (*TORC1, Ras/PKA,* and *Snf1*) that modulate *CaECM21* activity. Activated *CaECM21* facilitates Rsp5-dependent ubiquitination of *CaGAP1*, leading to transporter internalization and vacuolar degradation. *Rsp5-CaECM21* complex ubiquitinates CaGAP1, promoting endocytosis and transcription of *ART* genes, highlighting *CaECM21* as a central checkpoint integrating nutrient signaling, endocytic regulation, and antifungal stress adaptation.

3.6. Impact of Glucose and GlcNAc on *CaGap1* and Functional Assessment of *CaECM21*

Under YNB + glucose or GlcNAc, both strains exhibited weak CaGap1-GFP signals, indicating low *CaGap1* expression. In contrast, amino acid starvation (YNB W/O aa) enhanced *CaGap1* internalization, with pronounced vacuolar accumulation under GlcNAc, while glucose induced weaker internalization [Figure 7]. These observations indicate that *CaGap1* trafficking is strongly nutrient-dependent, with GlcNAc under amino acid starvation robustly promoting internalization, independent of *CaECM21*. Although the present study did not assess protein-protein interactions, future co-immunoprecipitation and ubiquitination assays will be instrumental in confirming the direct role of CaEcm21 as an adaptor for Rsp5-mediated transporter endocytosis.

3.7. Effect of GlcNAc-Induced Expression of *CaGap1*

In YNB-GlcNAc medium, in both wild-type and mutant strains, *CaGap1* is mainly localized in the cell membrane, as in YNB W/O aa GlcNAc medium, pFA-GFP*s* (BWP17) majorly shows its localization signal at the vacuole. These results indicate that *CaGap1* localizes to the plasma membrane in the presence of amino acids (YNB-GlcNAc medium), consistent with its role in aa uptake. To observe the internalization expression of *CaGAP1*, both wild-type and mutant strains were induced in YNB complete and YNB W/O aa. Fluorescence images were captured at 60 min and 120 min, respectively. Both wild type and mutant induced with YNB-GlcNAc, indicating low signal. Impressively, YNB W/O aa-GlcNAc induced wild-type cells show more internalization signal at the vacuole compared to the mutant [Figure 8].

3.8. Sensitivity to Amp B

In contrast, exposure to Amp B produced a clear, concentration-dependent growth inhibition pattern [Figure 9]. While wild-type and complemented strains exhibited normal tolerance, Δ/Δ*Caecm21* displayed hypersensitivity at both 0.7 µg/mL and 12 µg/mL [$P < 0.05$, Table 5]. This increased sensitivity likely results from altered membrane composition or trafficking defects affecting stress adaptation. The observation links *CaECM21*-mediated endocytosis to the maintenance of plasma membrane integrity under antifungal stress, although the direct molecular mechanism remains to be established.

Table 5: Colony intensity of *Candida albicans* strains under different media conditions.

Strain+media	YNB+DMSO (WC) mean±SD (95% CI)	YNB+culture mean±SD (95% CI)	0.7 µg/mL mean±SD (95% CI)	12 µg/mL mean±SD (95% CI)
BWP17-Glucose	0±0 (0, 0)	270.8±54.7 (232.1, 309.5)	224.0±38.9 (199.3, 248.7)	0±0 (0, 0)
BWP17-GlcNAc	0.75±1.5 (−1.7, 3.2)	290.8±59.0 (249.6, 332.0)	235.3±38.6 (210.7, 259.9)	0±0 (0, 0)
Δ/ΔCaecm21-Glucose	0±0 (0, 0)	209.8±79.0 (153.6, 266.0)	167.5±60.0 (125.9, 209.1)	0±0 (0, 0)
Δ/ΔCaecm21-GlcNAc	0.75±1.5 (−1.7, 3.2)	240.3±72.0 (190.4, 290.2)	189.3±73.0 (138.4, 240.2)	0±0 (0, 0)
ΔCaecm21-Glucose	0±0 (0, 0)	252.8±49.0 (218.7, 286.9)	191.5±49.0 (157.4, 225.6)	0±0 (0, 0)
ΔCaecm21-GlcNAc	0.75±1.5 (−1.7, 3.2)	264.3±49.0 (230.2, 298.4)	207.5±45.0 (176.7, 238.3)	0±0 (0, 0)

SD: Standard deviation, CI: Confidence interval, DMSO: Dimethyl sulfoxide.

4. CONCLUSION

This study focused on nutrient adaptation and revealed that *CaECM21* (ORF19.4887) functions as a novel ART adaptor protein in Candida albicans. Integrated *in silico*, and molecular analysis show that *CaECM21* regulates the endocytic turnover of nutrient transporter, *CaGAP1*. The Δ/Δ*CaECM21* mutant exhibited reproducible growth defects under nutrient-limited conditions and increased sensitivity to amphotericin B, linking ART-mediated endocytosis to stress adaptation.

Functional characterization revealed that *CaECM21* is required for proper localization of transporter, *CaGAP1* and internalization under YNB–GlcNAc and W/O-aa conditions, whereas no major defect was observed in YNB–glucose. These findings provide the first experimental evidence connecting *CaGAP1* internalization with *CaECM21* function in *C. albicans*, thereby expanding the understanding of ART-mediated endosomal trafficking in this pathogen. Notably, *CaECM21* deletion did not affect hyphal morphogenesis under the tested conditions, indicating a specific role in transporter trafficking and stress tolerance rather than global morphogenetic regulation.

The Δ/Δ*CaECM21* displayed enhanced susceptibility to Amp B in a concentration-dependent manner, supporting a functional link between endocytic trafficking and membrane stress response. Although the molecular mechanism remains to be elucidated, future studies involving co-immunoprecipitation and ubiquitination assays will probably clarify the interaction network underlying *CaECM21*-mediated regulation.

Collectively, these results establish *CaECM21* as a regulatory component of the fungal endocytic network that coordinates adaptive trafficking under nutrient limitation. By modulating the turnover of *CaGAP1*, *CaECM21* provides mechanistic insight into the integration of carbon and nitrogen metabolism, a process critical for survival and potential virulence in fluctuating host environments. The presence of conserved PPxY motifs further supports its function as an ART-like adaptor. The relatively modest phenotypes observed may reflect functional redundancy among paralogous ART adaptors that partially compensate for *CaECM21* deletion. This study mainly focused on *CaECM21* as a regulatory component of the endocytic network that integrates nutrient sensing with transporter turnover and antifungal stress adaptation in *C. albicans*, as illustrated in Figure 10.

4.1. Future Perspective

Future investigations should aim to define the molecular basis of *CaECM21*–Rsp5 interactions and identify the specific cargo proteins regulated through this pathway. Expanding this analysis to additional ART-domain proteins may uncover a broader regulatory network governing plasma membrane transporter composition and nutrient adaptation in Candida albicans. Although, this study primarily characterized *CaECM21*-mediated regulation of *CaGAP1*, it opens avenues for testing whether other nutrient transporters are similarly controlled by this adaptor, providing a framework for understanding transporter specificity versus generality within the ART family.

Further studies using infection models are necessary to evaluate the contribution of *CaECM21* to virulence and host–pathogen interactions. Comprehensive genetic analyses will be required to dissect redundancy within the ART network. From a therapeutic perspective, ART adaptors such as *CaECM21* represent potential antifungal targets. Interfering with ART-mediated endocytosis may impair nutrient acquisition and stress adaptation, thereby enhancing antifungal susceptibility. Detailed biochemical and structural characterization will be essential to define *CaECM21* interaction interfaces and assess its suitability as a selective antifungal target.

5. ACKNOWLEDGMENTS

The authors thank the Department of Science and Technology/SERB (CRG/2022/008507), Government of India, for providing financial support. KHR acknowledges a GITAM: Research Seed Grant, Gandhi Institute of Technology and Management (GITAM), Visakhapatnam, India. The author thanks the members of his laboratory at GITAM and the members of Dr. Swagata Ghosh's laboratory at the University of Kalyani, India, for their helpful suggestions.

6. CONFLICT OF INTEREST

The authors report no financial or any other conflicts of interest in this work.

7. AUTHOR'S CONTRIBUTIONS

All authors made substantial contributions to conception and design, acquisition of data, or analysis and interpretation of data; took part in drafting the article or revising it critically for important intellectual content; agreed to submit to the current journal; gave final approval of the version to be published; and agree to be accountable for all aspects of the work. All the authors are eligible to be author as per the International Committee of Medical Journal Editors (ICMJE) requirements/guidelines.

8. ETHICAL APPROVAL

Candida experiments were conducted as per guidelines. The study protocol was approved by the Institutional Biosafety Committee, GITAM School of Sciences, GITAM University, Visakhapatnam, India (Approval No. IAC/GU-1287-1287/HR-F/4; Date: 09.12.2023).

9. DATA AVAILABILITY

All the data is available with the authors and shall be provided upon request.

10. PUBLISHER'S NOTE

All claims expressed in this article are solely those of the authors and do not necessarily represent those of the publisher, the editors and the reviewers. This journal remains neutral with regard to jurisdictional claims in published institutional affiliation.

11. USE OF ARTIFICIAL INTELLIGENCE (AI)-ASSISTED TECHNOLOGY

The authors declare that they have not used artificial intelligence (AI)-tools for writing and editing of the manuscript, and no images were manipulated using AI.

REFERENCES

1. Wisplinghoff H, Bischoff T, Tallent SM, Seifert H, Wenzel RP, Edmond MB. Nosocomial bloodstream infections in US hospitals: Analysis of 24,179 cases from a prospective nationwide surveillance study. Clin Infect Dis. 2004;39(3):309-17. https://doi.org/10.1086/421946
2. Pfaller MA, Diekema DJ. Epidemiology of invasive candidiasis: A persistent public health problem. Clin Microbiol Rev. 2007;20(1):133-63. https://doi.org/10.1128/CMR.00029-06
3. Lockhart SR, Chowdhary A, Gold JA. The rapid emergence of antifungal-resistant human-pathogenic fungi. Nat Rev Microbiol. 2023;21(12):818-32. https://doi.org/10.1038/s41579-023-00960-9
4. Vazquez JA. Optimal management of oropharyngeal and esophageal candidiasis in patients living with HIV infection. HIV AIDS (Auckl). 2010;2:89-101. https://doi.org/10.2147/hiv.s6660
5. Sudbery PE. Growth of *Candida albicans* hyphae. Nat Rev Microbiol. 2011;9(10):737-48. https://doi.org/10.1038/nrmicro2636
6. Lo HJ, Köhler JR, DiDomenico B, Loebenberg D, Cacciapuoti A, Fink GR. Nonfilamentous *C. albicans* mutants are avirulent. Cell. 1997;90(5):939-49. https://doi.org/10.1016/s0092-8674(00)80358-x
7. Ene IV, Brunke S, Brown AJP, Hube B. Metabolism in fungal pathogenesis. Cold Spring Harb Perspect Med. 2014;4(12):a019695. https://doi.org/10.1101/cshperspect.a019695
8. Brown AJP, Budge S, Kaloriti D, Tillmann A, Jacobsen MD, Yin Z, *et al.* Stress adaptation in a pathogenic fungus. J Exp Biol. 2014;217(Pt 1):144-55. https://doi.org/10.1242/jeb.088930
9. Alvarez FJ, Konopka JB. Identification of an N-acetylglucosamine transporter that mediates hyphal induction in *Candida albicans*. Mol Biol Cell. 2007;18(3):965-75. https://doi.org/10.1091/mbc.e06-10-0931
10. Naseem S, Min K, Spitzer D, Gardin J, Konopka JB. Regulation of hyphal growth and N-acetylglucosamine catabolism by two transcription factors in *Candida albicans*. Genetics. 2017;206(1):299-314. https://doi.org/10.1534/genetics.117.201491
11. Biswas S, Van Dijck P, Datta A. Environmental sensing and signal transduction pathways regulating morphopathogenic determinants of *Candida albicans*. Microbiol Mol Biol Rev. 2007;71(2):348-76. https://doi.org/10.1128/MMBR.00009-06
12. Ljungdahl PO, Daignan-Fornier B. Regulation of amino acid, nucleotide, and phosphate metabolism in *Saccharomyces cerevisiae*. Genetics. 2012;190(3):885-929. https://doi.org/10.1534/genetics.111.133306
13. Ramachandra S, Linde J, Brock M, Guthke R, Hube B, Brunke S. Regulatory networks controlling nitrogen sensing and uptake in *Candida albicans*. PLoS One. 2014;9(3):e92734. https://doi.org/10.1371/journal.pone.0092734
14. Baile MG, Guiney EL, Sanford, EJ, MacGurn, JA, Smolka, MB, Emr SD. Activity of a ubiquitin ligase adaptor is regulated by disordered insertions in its arrestin domain. Mol Biol Cell. 2019;30(25):3057-3072. https://doi.org/10.1091/mbc.E19-08-0451
15. Nikko E, Pelham HR. Arrestin-mediated endocytosis of yeast plasma membrane transporters. Traffic. 2009;10(12):1856-67. https://doi.org/10.1111/j.1600-0854.2009.00990.x
16. Hanumantha Rao K, Roy K, Konopka JB. N-acetylglucosamine transporter Ngt1 undergoes sugar-responsive endocytosis in *Candida albicans*. Mol Microbiol. 2022;117(3):429-49. https://doi.org/10.1111/mmi.14857
17. Nikko E, Pelham HRB. Arrestin-mediated endocytosis of yeast plasma membrane transporters.Traffic. 2009;10(11):1856-67. https://doi.org/10.1111/j.1600-0854.2009.00990.x
18. Lee IR, Lim J, Steen J, Koh TH, Choi J, Jang J, *et al*. Amino acid permeases and virulence in Cryptococcus neoformans. PLoS One. 2016;11(9):e0163919. https://doi.org/10.1371/journal.pone.0163919
19. Vaknin Y, Shadkchan Y, Levdansky E, Morozov M, Romano J, Osherov N. The pH signaling transcription factor PacC governs pathogenicity and drug resistance in *Aspergillus fumigatus* via conserved arrestin-like proteins. Eukaryot Cell. 2014;13(8):1090-101. https://doi.org/10.1128/EC.00079-14
20. Hanumantha Rao K, Roy K, Konopka JB. N-acetylglucosamine transporter Ngt1 undergoes sugar-responsive endocytosis in *Candida albicans*. Mol Microbiol. 2022;117(3):429-49. https://doi.org/10.1111/mmi.14857
21. Fonzi WA, Irwin MY. Isogenic strain construction and gene mapping in *Candida albicans*. Genetics 1993;134(3):717-28. https://doi.org/10.1093/genetics/134.3.717.
22. Naseem S, Gunasekera A, Araya E, Konopka JB. N-acetylglucosamine (GlcNAc) induction of hyphal morphogenesis and transcriptional responses in *Candida albicans* are not dependent on its metabolism. J Biol Chem. 2011;286(33):28671-80. https://doi.org/10.1074/jbc.M111.249854
23. Jones T, Federspiel NA, Chibana H, Dungan J, Kalman S, Magee BB, *et al*. The diploid genome sequence of *Candida albicans*. Proc Natl Acad Sci USA. 2004;101(19):7329-34. https://doi.org/10.1073/pnas.0401648101
24. Altschul SF, Gish W, Miller W, Myers EW, Lipman DJ. Basic local alignment search tool. J Mol Biol. 1990;215(3):403-10. https://doi.org/10.1016/S0022-2836(05)80360-2
25. Thompson JD, Higgins DG, Gibson TJ. CLUSTAL W: Improving the sensitivity of progressive multiple sequence alignment through sequence weighting, position-specific gap penalties and weight matrix choice. Nucleic Acids Res. 1994;22(22):4673-80.
26. Marchler-Bauer A, Bo Y, Han L, He J, Lanczycki CJ, Lu S, *et al*. CDD/SPARCLE: functional classification of proteins via subfamily domain architectures. Nucleic Acids Res. 2017;45(D1):D200-3. https://doi.org/10.1093/nar/gkw1129
27. Skrzypek MS, Binkley J, Binkley G, Miyasato SR, Simison M, Sherlock G. The *Candida* Genome Database (CGD): Incorporation of Assembly 22, systematic identifiers and visualization of high throughput sequencing data. Nucleic Acids Res. 2017;45(D1):D592-6. https://doi.org/10.1093/nar/gkw924
28. Noble SM, Johnson AD. Strains and strategies for large-scale gene deletion studies of the diploid human fungal pathogen *Candida albicans*. Eukaryot Cell. 2005;4(2):298-309. https://doi.org/10.1128/EC.4.2.298-309.2005
29. Gunasekera A, Alvarez FJ, Douglas LM, Wang HX, Rosebrock AP, Konopka JB. Identification of GIG1, a GlcNAc-induced gene in *Candida albicans* needed for normal sensitivity to the chitin synthase inhibitor nikkomycin Z. Eukaryot Cell. 2010;9(10):1476-83. https://doi.org/10.1128/EC.00178-10

30. Gerami-Nejad M, Berman J, Gale C. Cassettes for PCR-mediated construction of green, yellow, and cyan fluorescent protein fusions in *Candida albicans*. Yeast. 2001;18(9):859-64. https://doi.org/10.1002/yea.738
31. Dueñas-Santero E, Santos-Almeida A, Rojo-Dominguez P, del Rey F, Correa-Bordes J, Vázquez de Aldana CR. A new toolkit for gene tagging in *Candida albicans* containing recyclable markers. PLoS One. 2019;14(7):e0219715. https://doi.org/10.1371/journal.pone.0219715
32. Biswas S, Roy M, Datta A. N-acetylglucosamine-inducible CaGAP1 encodes a general amino acid permease which co-ordinates external nitrogen source response and morphogenesis in *Candida albicans*. Microbiology (Reading). 2003;149(9):2597-608. https://doi.org/10.1099/mic.0.26215-0
33. Kraidlova L, Schrevens S, Van Zeebroeck G, Van Dijck P. The *Candida albicans* GAP gene family encodes permeases involved in amino acid uptake and sensing. Eukaryot Cell. 2011;10(9):1219-29. https://doi.org/10.1128/EC.05026-11
34. Grela E, Zdybicka-Barabas A, Pawlikowska-Pawlega B, Cytryńska M. Modes of the antibiotic activity of amphotericin B against *Candida albicans*. Sci Rep. 2019;9:17029. https://doi.org/10.1038/s41598-019-53517-3
35. Niimi K, Niimi M. The mechanisms of resistance to echinocandin class of antifungal drugs. Japanese J Med Mycol. 2009;50(2):57-66. https://doi.org/10.3314/jjmm.50.057
36. Kavanagh K, Dowd S. Histatins: Antimicrobial peptides with therapeutic potential. J Pharma Pharmacol. 2004;56(3):285-289. https://doi.org/10.1211/0022357022971
37. Sahoo S, Sharma S, Singh MP, Singh SK, Vamanu E, Rao KH. Metabolic and phenotypic changes induced during N-acetylglucosamine signalling in the fungal pathogen *Candida albicans*. Biomedicines. 2023;11(7):1997. https://doi.org/10.3390/biomedicines11071997
38. Inglis DO, Arnaud MB, Binkley J, Shah P, Skrzypek MS, Wymore F, *et al*. The *Candida* genome database incorporates multiple *Candida* species: Multispecies search and analysis tools with curated gene and protein information for *Candida albicans* and Candida glabrata. Nucleic Acids Res. 2012;40(Database issue):D667-74. https://doi.org/10.1093/nar/gkr945
39. Shihan MH, Novo SG, Le Marchand SJ, Wang Y, Duncan MK. A simple method for quantitating confocal fluorescent images. Biochem Biophys Rep. 2021;25:100916. https://doi.org/10.1016/j.bbrep.2021.100916

How to cite this article:
Haseena S, Sharma S, Rao KH. *CaECM21 (ORF19.4887),* a novel arrestin-related trafficking adaptor involved in nutrient transporter endocytosis and stress adaptation of *CaGAP1* in *Candida albicans*. J Appl Biol Biotech 2026;14(3):173-185. DOI: 10.7324/JABB.2026.285493